

Structural and Biochemical Studies of Dihydrofolate Reductase from *Streptococcus pyogenes* as a Target for Antifolate Antibiotics

Behnoush Hajian¹, Jolanta Krucinska¹, Michael Martins², Narendran G-Dayanan¹,
Kishore Viswanathan¹, Sara Tavakoli², Dennis Wright¹

¹Department of Pharmaceutical Sciences, University of Connecticut, Storrs, CT 06269

²Department of Cellular and Molecular Biology, University of Connecticut, Storrs, CT
06269

Corresponding author: Dennis Wright, dennis.wright@uconn.edu

ABSTRACT

Streptococcus pyogenes, a *beta*-hemolytic bacterium, causes a wide spectrum of infections in human including pharyngitis, tonsillitis, scarlet fever, rheumatic fever, and necrotizing fasciitis. Streptococcal infections can also exist as co-infection with methicillin resistant *Staphylococcus aureus* (MRSA). Trimethoprim-sulfamethoxazole (TMP-SMX) combination has been used for treatment of *S. pyogenes* and MRSA co-infection. However, resistance to TMP, an inhibitor of dihydrofolate reductase enzyme (DHFR), has challenged the efficacy of TMP-SMX combination. We explored the activity of a series of novel DHFR inhibitors against *S. pyogenes*. This study identified potent inhibitors of DHFR enzyme from *S. pyogenes* with excellent inhibitory activity against the growth of the live bacteria. We determined, for the first time, the crystal structure of *S. pyogenes* DHFR which provides structural insights into design and development of antifolate agents against this global pathogen.

Key words: *Streptococcus pyogenes*, folate pathway, dihydrofolate reductase, trimethoprim, MRSA, antifolates

INTRODUCTION

Streptococcus pyogenes, or Lancefield's group A Streptococcus (GAS), is a Gram-positive bacterium that causes a diverse spectrum of human infections. Streptococcal infections are usually mild such as pharyngitis (strep throat) and impetigo. But if the infection reaches deeper tissues, it can cause invasive infections such as necrotizing fasciitis (flesh eating disease) and streptococcal toxic shock syndrome. Superficial GAS infections can be followed by abnormal immune responses which may result in post-streptococcal sequelae including acute rheumatic fever and acute post-streptococcal glomerulonephritis.¹ The prevalence of severe GAS infections is 18.1 million cases, with 1.78 new cases and 517 000 deaths each year. The past decade has witnessed a global resurgence of streptococcal diseases such as skin and soft tissue infections and scarlet fever.^{2,3}

Although, *S. pyogenes* in general remains susceptible to most classes of antibiotics, treatment of streptococcal infections is challenged by the rising tide of antimicrobial resistance (AMR).⁴⁻⁷ Over the past two decades, there has been an increasing rate of macrolide resistance among *S. pyogenes* isolates in Europe and worldwide.⁸⁻¹¹ There has been also a growing rate of penicillin failure mostly due to lack of penicillin permeation into the infected tissues and co-infection of *S. pyogenes* with beta-

lactamase producing bacteria such as *Staphylococcus aureus*.⁴

Trimethoprim-sulfamethoxazole combination (SXT), one of the most widely used and cheapest antibacterials in the world, is currently suggested as a valuable option for treatment of skin and soft tissue coinfections with *S. pyogenes* and methicillin-resistant *S. aureus* (MRSA), when penicillin treatment fails.¹² However, the emergence of trimethoprim (TMP) resistance in *S. pyogenes* isolates have challenged the efficacy of SXT.^{13,14} TMP is an inhibitor of dihydrofolate reductase (DHFR), one of the key enzymes in the folate biosynthetic pathway. The folate pathway is essential in the synthesis of reduced folates, the one-carbon donors required for the production of deoxythymidine monophosphate (dTMP), purine nucleotides, methionine and histidine (**Figure 1**). DHFR catalyzes the reduction of DHF to THF using NADPH as an electron donor. Due to its pivotal role in regulating cellular levels of THF and its derivatives, DHFR has served as an attractive target for many anticancer, antibacterial, and antiprotozoal drugs.^{15,16}

Herein, we report the activity of a series of propargyl-linked antifolates (PLAs) against *S. pyogenes* and DHFR enzyme from this pathogen (SpDHFR). Previously, we have shown that PLAs are inhibitors of TMP-susceptible and TMP-resistant MRSA isolates.¹⁷⁻²⁰ Screening of

PLAs against *S. pyogenes* identified a group of novel PLAs with pronounced antibacterial activity. Further exploration of structure activity relationship (SAR) of this group has led to the identification of potent inhibitors of SpDHFR enzyme.

Here we report for the first-time high resolution crystal structure of SpDHFR in a ternary complex with NADPH and one

of the lead PLAs which provides structural insights into the design of potent and selective inhibitors. Our data strongly support the effort to explore PLAs as promising candidate for design of novel antifolates against TMP-resistant *S. pyogenes* and MRSA coinfections.

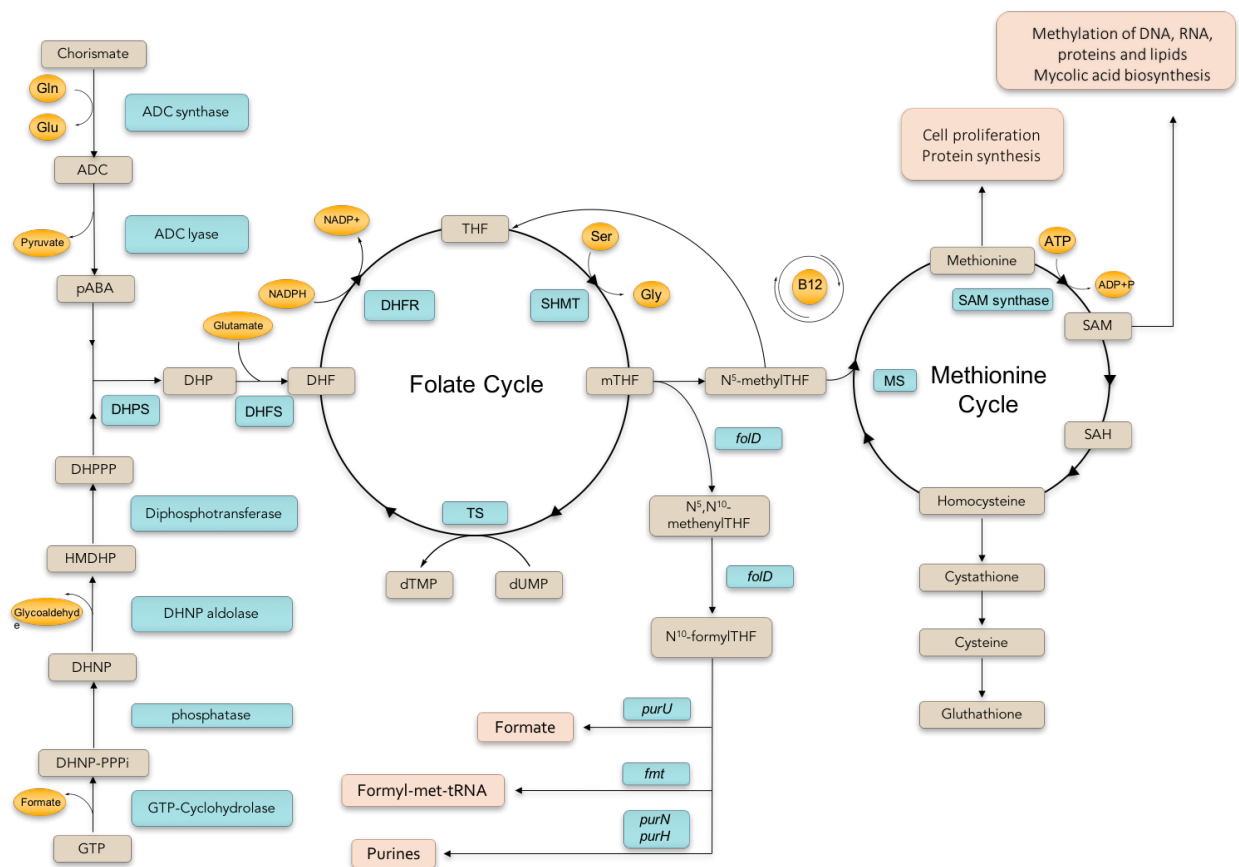


Figure 1. Bacterial folate cycle and related pathways. ADC: aminodeoxy chorismate, PABA: para-aminobenzoic acid, DHPPP: 7,8-dihydropterin pyrophosphate, HMDHP: 6-hydroxymethyl-7,8-dihydropterin, DHNP: 7,8-dihydroneopterine, DHNP-PPPi: 7,8-dihydroneopterine triphosphate, DHP: 7,8-dihydropteroate, DHF: 7,8-dihydrofolate, THF: 5,6,7,8-tetrahydrofolate, DHFR: dihydrofolate reductase, SHMT: serine hydroxymethyltransferase, mTHF: N⁵,N¹⁰-methyleneTHF, 5-mTHF: N⁵-methylTHF, TS: thymidylate synthase, MS: methionine synthase, SAM: S-adenosyl methionine, SAH: S-adenosyl homocysteine

RESULTS

Antimicrobial activity of PLAs against *S. pyogenes*. Using broth micro dilution

method, a series of PLAs were tested for their inhibitory activity against the growth of *S. pyogenes* ATCC 19615

(Rosenbach), a quality control strain used in a variety of susceptibility assays. PLASs scaffold includes a 2,4-diaminopyrimidine ring (ring A) linked to an aryl or heteroaryl system (ring B and C) through a propargyl bridge. Based on the variations in the B- and C-rings, the tested PLAs were categorized into six general groups (Table 1 and Table S1). With only one exception (compound 34), all the tested compounds exhibited very promising antimicrobial activity against *S. pyogenes* with MIC values below 1 µg/ml.

Inhibition of *S. pyogenes* DHFR enzyme by PLAs. To test whether the inhibitory activity of PLAs against *S. pyogenes* cells is mediated through the inhibition of DHFR enzyme, we evaluated the inhibitory effect of the compounds against the purified enzyme. The half maximal inhibitory concentrations (IC₅₀ values) are shown in Table 1. Although the potency of the compounds varies, in general there is a correlation between the enzyme and cell growth inhibition. SAR analysis of each group of the tested compounds elucidated key structural features that affect the potency of PLAs against SpDHFR.

Group one is characterized by PLA-COOH compounds which feature a carboxylic acid substitution on the C-ring. The IC₅₀ values observed in this category varies between 50 to 250 nM. Within this group, the presence of propargylic methyl correlates with a

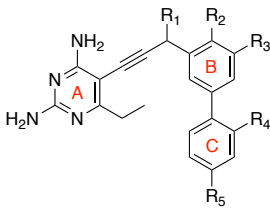
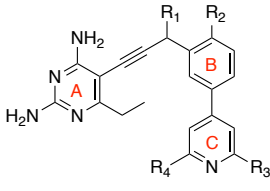
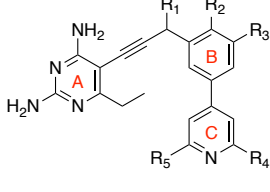
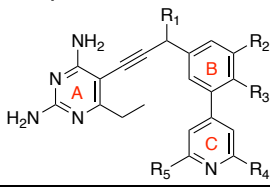
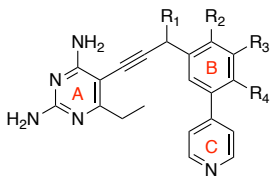
decrease in the potency of the compounds. As seen with compounds 1 and 7, the absence of propargylic methyl leads to improved inhibitory activity against SpDHFR (IC₅₀ values of 73 and 57 nM, respectively). In addition, moving the carboxylate from the *para* (in compound 7) to the *ortho* position (in compound 6) compromised the inhibitory effect by almost four-folds (IC₅₀ values of 57 and 200 nM, respectively). Furthermore, the stereoisomers of *S* configuration (compounds 2 and 4) exhibit similar activity with *R* isomers (compounds 3 and 5). The lack of apparent stereospecificity is continuously evident across all the other tested PLAs.

Compounds in group two feature a pyrimidine C-ring and a chlorine substitution at 2' position on the B-ring. Here, compound 8 is the most potent congener with IC₅₀ value of 85 nM. Introduction of two methyl groups on the C-ring (compound 10) leads to a modest decrease in inhibitory affinity (IC₅₀ value of 193 nM).

Based on the same concept, group three represents fluorine atoms substitution on the B-ring. IC₅₀ values for this group range from 40 to 350 nM. Not surprisingly, the presence of propargylic methyl and/or methyl substitutions on the C-ring reflects the same trend as seen with chlorine atom derivatives. Next we evaluated the effect of heterocyclic substitution on the B-ring by

introducing a dioxane and dioxalane moieties on the B-ring (Group four and five).

Table 1. Biological activity of PLAs against *S. pyogenes* and DHFR enzymes

Structures	ID	R ₁	R ₂	R ₃	R ₄	R ₅	X ₁	X ₂	X ₃	n	SpDHFR IC ₅₀ (nM)	MIC (µg/mL)	HuDHFR IC ₅₀ (nM)
	1	H	H	OCH ₃	H	COOH	-	-	-	-	73 ± 5	≤0.039	688 ± 12
	2	S-CH ₃	H	OCH ₃	H	COOH	-	-	-	-	142 ± 8	≤0.039	400 ± 20
	3	R-CH ₃	H	OCH ₃	H	COOH	-	-	-	-	250 ± 8	≤0.039	502 ± 15
	4	S-CH ₃	OCH ₃	H	H	COOH	-	-	-	-	226 ± 12	0.078	520 ± 14
	5	R-CH ₃	OCH ₃	H	H	COOH	-	-	-	-	185 ± 9	0.078	266 ± 15
	6	H	OCH ₃	H	COOH	H	-	-	-	-	200 ± 16	0.625	3547 ± 230
	7	H	OCH ₃	H	H	COOH	-	-	-	-	57 ± 5	0.078	870 ± 22
	8	CH ₃	Cl	H	H	-	-	-	-	-	85 ± 4		ND
	9	S-CH ₃	Cl	CH ₃	CH ₃	-	-	-	-	-	243 ± 12	≤0.039	210 ± 18
	10	CH ₃	Cl	CH ₃	CH ₃	-	-	-	-	-	193 ± 16	0.312	ND
	11	R-CH ₃	Cl	CH ₃	CH ₃	-	-	-	-	-	375 ± 21	0.625	207 ± 13
	12	S-CH ₃	OCF ₃	H	CH ₃	CH ₃	-	-	-	-	354 ± 25	0.312	ND
	13	R-CH ₃	OCF ₃	H	CH ₃	CH ₃	-	-	-	-	288 ± 22	0.156	167 ± 9
	14	H	OCF ₃	H	CH ₃	CH ₃	-	-	-	-	212 ± 18	0.625	ND
	15	CH ₃	OCF ₃	H	CH ₃	CH ₃	-	-	-	-	157 ± 13	0.312	ND
	16	CH ₃	H	F	CH ₃	CH ₃	-	-	-	-	41 ± 5	≤0.039	ND
	17	CH ₃	OCH ₃	F	H	H	-	-	-	-	42 ± 3	≤0.039	234 ± 16
	18	CH ₃	H	H	CH ₃	CH ₃	-	-	-	-	132 ± 12	≤0.039	ND
	19	CH ₃	3',4'-dioxane		CH ₃	CH ₃	-	-	-	-	172 ± 23	≤0.039	ND
	20	CH ₃	3',4'-dioxane		H	H	-	-	-	-	211 ± 11	≤0.039	290 ± 16
	21	S-CH ₃	H	3',4'-dioxolane			-	-	-	-	38 ± 5	≤0.039	191 ± 12
	22	R-CH ₃	H	3',4'-dioxolane			-	-	-	-	74 ± 4	≤0.039	85 ± 10
	23	S-CH ₃	H	H	OCH ₃			-	-	-	207 ± 12	≤0.039	68 ± 7
	24	R-CH ₃	H	H	OCH ₃			-	-	-	163 ± 14	≤0.039	74 ± 7
	25	S-CH ₃	OCH ₃	H	H			-	-	-	42 ± 4	≤0.039	232 ± 21
	26	R-CH ₃	OCH ₃	H	H			-	-	-	31 ± 4	≤0.039	144 ± 17

	27	S-CH ₃	H	OCH ₃	H	-	-	-	-	-	33 ± 5	≤0.039	366 ± 23
	28	R-CH ₃	H	OCH ₃	H	-	-	-	-	-	43 ± 4	≤0.039	516 ± 31
	29	CH ₃	H	OCH ₃	OCH ₃	-	-	-	-	-	35 ± 6	≤0.039	362 ± 18
	30	R-CH ₃	H	OCH ₃	OCH ₃	-	-	-	-	-	95 ± 5	≤0.039	206 ± 21
	31	CH ₃	2',3'-dioxolane		H	-	-	-	-	-	9 ± 3	≤0.039	201 ± 16
	32	CH ₃	H	OH	OH	-	-	-	-	-	451 ± 24	0.312	ND
Group 6 	33	H	-	-	-	-	-	-	N	-	129 ± 9	≤0.039	1133 ± 175
	34	OH	-	-	-	-	N	-	N	-	647 ± 32	2.5	ND
	35	CH ₃	CH ₃	-	-	-	N	N	-	-	120 ± 13	≤0.039	ND

Interestingly, the presence of 3',4'-dioxane (compounds **19** and **20**) has minimal effect on the potency of PLAs (IC₅₀ values of 132 and 172 nM). By contrast, 3'-4'-dioxalane substitution (compound **21** and **22**) resulted in enhance inhibitory activity by as much as five-fold.

These observations prompted us to investigate different B-ring modifications in the context of substituted and unsubstituted B-ring (group five). Moving the dioxolane substitution from 3',4' to 2',3' position yielded compound **31**, superior in both potency and selectivity, with IC₅₀ value of 9 nM. These structural analysis highlights the importance of a simple change around the B-ring at 2', 3', and 4' position on the potency and affinity of these compounds against SpDHFR.

Group six represent three compounds with *para* C-ring and various nitrogen substitutions on B- and C-rings. These

compounds have moderate inhibitory activity with IC₅₀ values above 100 nM. It is notable that replacement of the propargylic methyl with a hydroxyl moiety (compound **34**) is not tolerated (IC₅₀ value of ~650 nM). Selectivity over the human form of DHFR, to ensure low toxicity, is an important parameter to consider. We have measured the inhibitory effect of select compounds against the human DHFR enzyme (HuDHFR) and reported it as IC₅₀ values (Table 1).

In summary, compounds lacking propargylic substitution (compounds **1** and **7**) and/or those without bulky substitutions on the C-ring yielded more selective compounds. The main structural variations that drive the potency and selectivity of PLAs against SpDHFR appear to be the simplified propargyl, 2', and 3' substitution on the B-ring as well as meta-substitution on the C-ring.

HuDHFR	MVGS LNCIVAVSQ NMGIGKNGDLPW PPLRNEFRYFQRM TTSS VEGKQNLVIMGKKTWFS	60
MtbDHFR	-MTMVGLIWAQATSGVIGRGGDIPWR-LPEDQAHFREITM-----GHTIVMGRRTWDS	51
SpDHFR	MTKEIIAIWAED EAGLIGVAGKLPWY -LPKEL EHFK KTTL-----HQAILMGRVTFEG	52
SpnDHFR	MTKKIVAIAQDEEGVIGKENR LPWH -LPAELQHFKETTL-----NHAILMGRVTFDG	52
SaDHFR	--MTLSILVAHDLQRVIGFENQLPWH-LPNDLKHVKKLS T -----GHTLVMGRKTFES	50
EcDHFR	---MISLIAALAVDRVIGMENAMPWN-LPADLAWFKRNTL-----NKPVIMGRHTWES	49
HuDHFR	IPEK NRPLKGRINLVLSREL KEPPQGAHFLSRS LDDAL KLTEQPELANKVDMVWIVGGSS	120
MtbDHFR	LP AKVRPLP GRRNVVLSRQADFMASGAEVVG-SLEEAL-----TSPETWVIGGGQ	100
SpDHFR	MN--CKRLPQRQTLV MTRN RDYQVDEVLTMT-SIEKVLEWY----HAQDKTLYIIGGNK	104
SpnDHFR	MG--RRLLPKRETLILTRNPEEKIDGVATFQ-DVQSVLDWY----QAQEK NLYIIGGK Q	104
SaDHFR	IG--K-PLPNRRNVV LTS DTSFNVEGVDVIH-SIEDIY-----Q-LPGHVFI FGGQ T	97
EcDHFR	IG--R-PLPGRKNII LSSQ PGTDDR-VTWVK-SVDEAIAAC----G-DVPEIMVI GGGR	98
HuDHFR	VYKEAMNHPGHLKLFVTRIMQDF---ESD TFFP -EIDLEKYKLLPEYPGVLSDVQEEKGI	176
MtbDHFR	VYALALPY--ATRCEVTEVDIGL PREAGDALAP -VL-DETWRGET---GEWFRS RSL --	151
SpDHFR	VLEAFNGY--FDRIIKTVI HHRF ---KGD TYRP -NLDFSHFTQES---QTFYARDAKNPY	155
SpnDHFR	IFQAFEPY--LDEVIVTHI HARV ---EGD TYFPEEL DL SLF ETVS---SKFYAKDEKNPY	156
SaDHFR	LF EEM IDK--VDDMYITVIEGKF---RGD TFFP -PYTFEDWEVAS---SVEGKLD EKNTI	148
EcDHFR	VYEQFLPK--AQKLYLTHIDAEV---EGD THFP -DYEPDDWESVF---SEPHDADAQNSH	149
HuDHFR	KYKFEVYEKND- 187 (Sequence homology with SpDHFR: 29%)	
MtbDHFR	RYRLYSYHRS-- 161 (Sequence homology with SpDHFR: 29%)	
SpDHFR	DFTVTALKHK-- 165	
SpnDHFR	DFTIQRKRKEV 168 (Sequence homology with SpDHFR: 56%)	
SaDHFR	PHTFLHLIRKK- 159 (Sequence homology with SpDHFR: 33%)	
EcDHFR	SYCFEILERR-- 159 (Sequence homology with SpDHFR: 26%)	

Figure 2. Sequence alignment of SpDHFR with other known DHFR enzymes. Folate binding site residues are shown in red. Cofactor binding site residues are shown in blue. **Hu:** *Homo sapiens*, **Mtb:** *Mycobacterium tuberculosis*, **Spn:** *Streptococcus pneumoniae*, **Sa:** *Staphylococcus aureus*, and **Ec:** *Escherichia coli*

Enzyme Structural Analysis. To investigate drug-target interactions, we have successfully crystalized SpDHFR in complex with compound **3**. The X-ray crystal structure of SpDHFR bound to cofactor NADPH and the ligand was determined at 2.2 Å with the final R-factor of 0.19 and R_{free} of 0.25 (Table S1). The crystal belongs to the orthorhombic space group $P2_12_12_1$ with four molecules in the asymmetric unit. Despite low sequence homology with DHFR enzymes (Figure 2), SpDHFR structure exhibit the same general fold composed of a central β -sheet and four flanking α -helices (Figure 3 A and B). SpDHFR is composed of eight parallel β -strands (β 1, β 2, β 3, β 4, β 5, β 6, β 7, and β 9), two anti-parallel β -strands (β 8 and β 10), and four α -helices (α 1, α 2, α 3, and α 4). Full

density for both NADPH and compound **3** was also observed (Figure 4A).

NADPH binding site. The NADPH molecule is bound to SpDHFR in an extended conformation with the nicotinamide ring inserted into a cleft formed by β 1, β 2, and β 8-strands (Figures 3A and 4A). NADPH is anchored into the cofactor binding pocket through extensive interactions with the active site residues (Figure 4B). The amide group of the nicotinamide ring forms three hydrogen bonds with the backbone of Ala10 and Ile17. The nicotinamide ribose contacts Val19, Gly21, and Lys22. The pyrophosphate moiety interacts extensively with the residues from α 2 and α 4 helices (Val48, Thr49, Asn103, and Lys104). The O2'-phosphate of adenosyl ribose forms

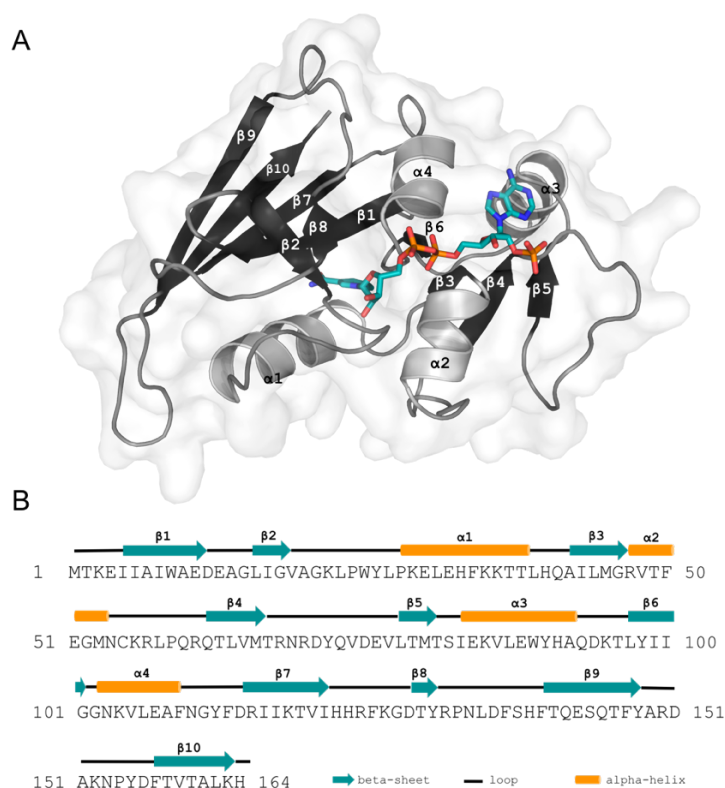


Figure 3. Structure of SpDHFR and assignment of secondary structures. A) Schematic ribbon diagram of the overall fold of SpDHFR. NADPH is shown using a stick model. B) Assignment of secondary structures for SpDHFR sequence.

four hydrogen bonds with Arg47, Thr67, and Arg68. The adenine group contacts the protein through interactions with Thr81 and Ser82 and stacking against Met66.

Folate binding site. The 2,4-diaminopyrimidine ring of compound **3** is deeply positioned into the hydrophobic binding pocket and forms two hydrogen bonds with Glu30 and another hydrogen bond with the backbone carboxylate of Ile8 (Figures 4A and 4C). Glu30 is highly conserved and critical for the catalytic activity of DHFR. In some species, this

residue is replaced by Asp which provides similar interactions (Figure 2). There are also water-mediated interactions between the 2,4-diaminopyrimidine ring of compound **3** and the residues in the binding pocket and π - π stacking with Phe34. This arrangement around the diaminopyrimidine ring is highly conserved among the known DHFR structures from various species. The biaryl moiety of compound **3** makes hydrophobic interactions with Ile100, Thr49, Phe50, Met53, and Leu58. The carboxylate of compound **3** has a weak electrostatic

ligand²² (Figure 5B), it becomes evident that the interactions of the 2,4-diaminopyrimidine ring that anchors compound **3** in the active site are almost identical.

Despite the similarities, there are several structural variations that can be exploited for design of selective inhibitors. For example, replacement of Phe31 in HuDHFR by corresponding residue Leu31 in SpDHFR provides greater van der Waals interactions in SpDHFR while the larger group likely contribute to destabilizing

interactions in HuDHFR. Another notable difference is Pro61 in HuDHFR which corresponds to Asn54 in SpDHFR. Inhibitors with polar substitutions that can advantage from contacts with Asn54 may bind selectively to SpDHFR. An analog of compound **3** with a hydrogen bond donor on the C-ring or a hydrophilic group added to the B-ring may provide an excellent chemical space to explore. Still, a consideration should be given to the size, position, and character of these additional moieties as seen from our SAR analysis.

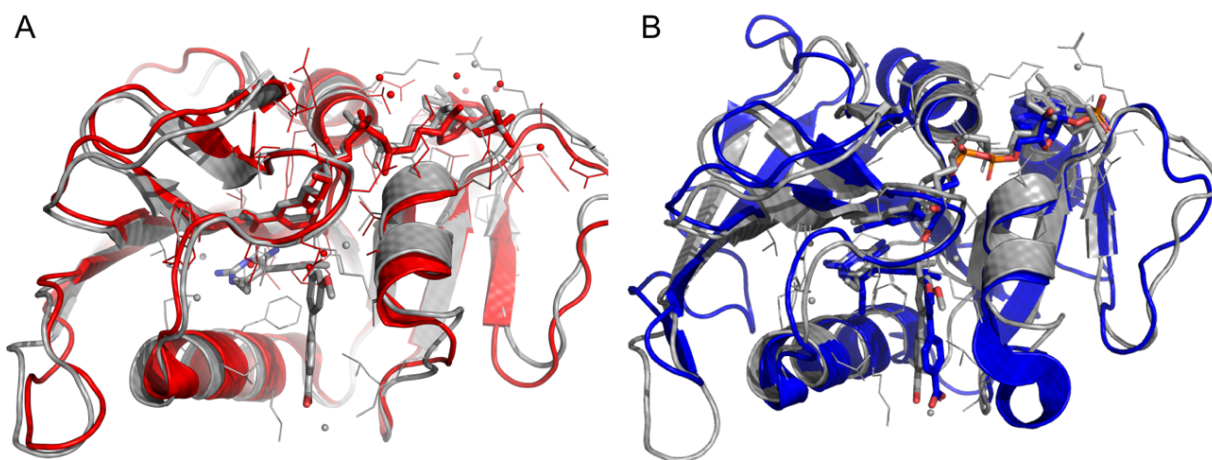


Figure 5. A) Superposition of SpDHFR (gray) and SaDHFR (red), B) Superposition of SpDHFR (grey) and HuDHFR (blue)

CONCLUSION

The results presented in this work, provide insights into the structure-based design of inhibitors of DHFR in *S. pyogenes*. DHFR inhibitors have been widely used as effective anticancer and antibacterial agents.^{15,23} However, resistance to TMP,

one of the most effective DHFR inhibitors, has challenged the efficacy of this drug as an antibacterial agent. TMP, often in combination with SMX, is used for treatment of skin, urinary tract, and enteric infections caused by Gram-positive and

Gram-negative bacteria.²⁴⁻²⁶ *S. pyogenes* causes million cases of human infections every year and its capacity to develop invasive infections emphasizes the need for global control of streptococcal infections. Common co-infection of *S. pyogenes* and MRSA and difficulties in distinguishing between the two, highlights the importance of developing therapeutics with activity against both pathogen and ideally TMP-resistant isolates. Previously, we have reported a series of DHFR inhibitors with activity against TMP-sensitive and TMP-

resistant MRSA isolates.¹⁷⁻²⁰ Here, we have shown that these compounds maintain their inhibitory activity against DHFR enzyme from *S. pyogenes* and the growth of live bacteria. SAR analysis of the tested compounds along with determining the structure of SpDHFR in complex with one of the lead compounds provide key structural information required for optimization of dual inhibitors of both pathogen.

METHODS

Antimicrobial agents. The synthesis and characterization of PLAs have been described in several publications. Trimethoprim (TMP) was purchased from Sigma Chemical Co., St. All the compounds were dissolved in 100% dimethyl sulfoxide (DMSO) prior to use.

Bacterial isolate. *S. pyogenes* ATCC 19615 was purchased from the American Type Culture Collection (Manassas, VA). The organism was grown in Todd Hewitt broth.

In vitro susceptibility testing. The assay was performed in Isosensitest broth (Oxoid) supplemented with 5% defibrinated sheep blood (ThermoFisher). Minimum inhibitory concentrations (MIC) were determined by broth microdilution method based on CLSI guideline using a final inoculum of 5×10^5 CFU/ml. The antimicrobial agents were prepared at 40 µg/ml and were dispensed using serial two-fold dilution. The MIC was defined as the lowest concentration of antimicrobial agent yielding no visible growth after monitoring cell turbidity following an incubation period of 24-36 hours at 37°C.

Transformation, expression, and purification of SpDHFR. Recombinant pET-24a(+) plasmid harboring the *folA* gene encoding SpDHFR was constructed by GenScript. BL21(DE3) competent *E. Coli* cells (New England BioLabs) were transformed with the recombinant plasmids. Transformed cells were grown in LB medium supplemented with 30 µg/mL kanamycin at 37°C until OD₆₀₀ reached 0.6-0.7. The cells were induced with 1 mM IPTG for 20 hours at 20°C and spun down at 8000 rpm for 15 minutes. Each gram of wet cell pellet was resuspended in 5 ml of lysis buffer (25 mM Tris pH 8.0, 0.4 M KCl, 5 mM imidazole, 5 mM BME, 5% glycerol, 200 µg/ml lysozyme, 1 mM DNase I). The cell suspension was incubated for 30-60 minutes at 4°C with gentle rotation followed by sonication until a homogenous lysate was obtained. The lysate was centrifuged at 18,000 rpm for 30 minutes and supernatant was collected and filtered through 0.22 µm filter. The SpDHFR construct did not contain histidine tag and were purified over methotrexate-agarose column pre-equilibrated with 4 CV of equilibration buffer (20mM Tris-HCl pH 7.5, 50 mM KCl, 2 mM DTT, 0.1 mM EDTA and 15% glycerol). The column was washed with 3 CV of wash buffer (20 mM Tris-HCl pH 7.5, 500 mM KCl, 2 mM DTT, 0.1 mM EDTA and 15% glycerol). The protein was eluted with 3 CV of elution buffer (equilibration buffer pH 8.5 + 2mM DHF). Fractions containing SpDHFR protein were collected, concentrated and loaded onto a Hi-Prep 26/60 Sephacryl s-200 HR prepacked gel filtration/size exclusion column pre-equilibrated with 1 CV of final buffer (25 mM Tris pH 8.0, 50 mM KCl, 0.1 mM EDTA, 2 mM DTT and 15% glycerol). The column was washed with another 1 CV of final buffer and protein elution was monitored with AKTA UV/vis diode array spectrophotometer at 280 nm. Fractions containing pure enzyme

were pooled, concentrated at 10 mg/ml and flash frozen in liquid nitrogen and stored at -80°C.

Enzyme inhibition assay. The DHFR activity of SpDHFR was measured in 500 µl of assay buffer containing 20 mM TES, 50 mM KCl, 0.5 mM EDTA, 10 mM 2-mercaptoethanol (BME) and 1 mg/ml bovine serum albumin (BSA) with various concentrations of NADPH and DHF ranging from 0 to 100 µM. Assay was started by adding DHF and monitoring NADPH oxidation at 340 nm. All measurements were performed at room temperature and in triplicates. Initial velocity data were fitted with the Michaelis-Menten equation using Graphpad Prism 7.0 software. The DHFR activity inhibition assays and IC₅₀ determination were performed in the same assay buffer with 100 µM NADPH and 100 µM DHF. Inhibitors, dissolved in 100% DMSO, were added to the mixture and incubated for 5 minutes before the addition of DHF. Average IC₅₀ values and standard deviations were measured in triplicate.

Crystallization of SpDHFR. All the crystallization trials were performed by hanging drop vapor diffusion method and using EasyXtal 15-well plates (Qiagen). SpDHFR was mixed with 10 mM NADPH and 2mM ligand, incubated on ice for two hours and concentrated to 14 mg/mL. 2 µl of this solution was mixed with 2 µl of crystallization solution containing 50-150 mM sodium cacodylate pH 6-7, 200 mM magnesium acetate, and 20-30% of polyethylene glycol 3350. Small polygonal crystals grew within 2-3 weeks at 4°C. Crystals were flash frozen in the mother liquor supplemented with 20% glycerol.

Data collection and structure determination. X-ray data were collected at National Synchrotron Light Source II (NSLS II) at Brookhaven National Laboratory. Data were integrated using iMOSFLM and scaled and merged using AIMLESS from CCP4i2 suite. Molecular replacement was performed using Phaser and previously reported structure of DHFR from *S. pneumoniae* sharing ~50% sequence identity with SpDHFR. The structure was refined using Coot and Phenix softwares.

REFERENCES

1. Barnett, T. C., Bowen, A. C. & Carapetis, J. R. Epidemiology and Infection The fall and rise of Group A Streptococcus diseases. (2018). doi:10.1017/S0950268818002285
2. Carapetis, J. R., Steer, A. C., Mulholland, E. K. & Weber, M. The global burden of group A streptococcal diseases. *Lancet Infect. Dis.* **5**, 685–694 (2005).
3. Wong, S. S. & Yuen, K.-Y. Streptococcus pyogenes and re-emergence of scarlet fever as a public health problem. (2012). doi:10.1038/emi.2012.9
4. PassÀli, D., lauriello, M., PassÀli, G. & PassÀli, F. *Group A Streptococcus and its antibiotic resistance Lo Streptococco beta-emolitico di gruppo A e la sua resistenza alla terapia antibiotica.*
5. Arvand, M., Hoeck, M., Hahn, H. & Wagner, J. Antimicrobial resistance in Streptococcus pyogenes

- isolates in Berlin. *J. Antimicrob. Chemother.* **46**, 621–624 (2000).
6. Passàli, D., Lauriello, M., Passàli, G. C., Passàli, F. M. & Bellussi, L. Group A streptococcus and its antibiotic resistance. *Acta Otorhinolaryngol. Ital.* **27**, 27–32 (2007).
 7. Cattoir, V. *Mechanisms of Antibiotic Resistance. Streptococcus pyogenes: Basic Biology to Clinical Manifestations* (University of Oklahoma Health Sciences Center, 2016).
 8. Reinert, R. R., Lütticken, R., Bryskier, A. & Al-Lahham, A. Macrolide-resistant *Streptococcus pneumoniae* and *Streptococcus pyogenes* in the pediatric population in Germany during 2000–2001. *Antimicrob. Agents Chemother.* **47**, 489–93 (2003).
 9. Van Heirstraeten, L. et al. Antimicrobial drug use and macrolide-resistant *Streptococcus pyogenes*, Belgium. *Emerg. Infect. Dis.* **18**, 1515–8 (2012).
 10. Bingen, E. et al. Emergence of macrolide-resistant *Streptococcus pyogenes* strains in French children. *Antimicrob. Agents Chemother.* **48**, 3559–62 (2004).
 11. Silva-Costa, C., Friães, A., Ramirez, M. & Melo-Cristino, J. Macrolide-resistant *Streptococcus pyogenes*: prevalence and treatment strategies. *Expert Rev. Anti. Infect. Ther.* **13**, 615–628 (2015).
 12. Bowen, A. C. et al. Is *Streptococcus pyogenes* resistant or susceptible to trimethoprim-sulfamethoxazole? *J. Clin. Microbiol.* **50**, 4067–72 (2012).
 13. Bergmann, R., van der Linden, M., Chhatwal, G. S. & Nitsche-Schmitz, D. P. Factors that cause trimethoprim resistance in *Streptococcus pyogenes*. *Antimicrob. Agents Chemother.* **58**, 2281–8 (2014).
 14. Bergmann, R., Sagar, V., Nitsche-Schmitz, D. P. & Chhatwal, G. S. first detection of trimethoprim resistance determinant *dfgG* in *Streptococcus pyogenes* clinical isolates in India. *Antimicrob. Agents Chemother.* **56**, 5424–5 (2012).
 15. Scocchera, E. & Wright, D. L. in 1–27 (Springer, Berlin, Heidelberg, 2017). doi:10.1007/7355_2017_16
 16. Kompis, I. M., Islam, K. & Then, R. L. DNA and RNA synthesis: Antifolates. *Chem. Rev.* **105**, 593–620 (2005).
 17. Scocchera, E. et al. Charged Nonclassical Antifolates with Activity Against Gram-Positive and Gram-Negative Pathogens. *ACS Med. Chem. Lett.* **7**, 692–696 (2016).
 18. Keshipeddy, S., Reeve, S. M., Anderson, A. C. & Wright, D. L. Nonracemic Antifolates Stereoselectively Recruit Alternate Cofactors and Overcome Resistance in *S. aureus*. *J. Am. Chem. Soc.* **137**, 8983–8990 (2015).
 19. Reeve, S. M. et al. MRSA Isolates from United States Hospitals Carry *dfgG* and *dfgK* Resistance Genes and Succumb to Propargyl-Linked Antifolates. *Cell Chem. Biol.* **23**, (2016).
 20. Reeve, S. M. et al. Charged Propargyl-Linked Antifolates Reveal Mechanisms of Antifolate Resistance and Inhibit Trimethoprim-Resistant MRSA Strains Possessing Clinically Relevant Mutations. *J. Med. Chem.* **59**, 6493–6500 (2016).
 21. Reeve, S. M. et al. Protein design algorithms predict viable resistance to an experimental antifolate. *Proc. Natl. Acad. Sci. U. S. A.* **112**, 749–54 (2015).
 22. Hajian, B. et al. Drugging the Folate Pathway in Mycobacterium Tuberculosis: The Role of Multi-Targeting Agents. (2018).
 23. Visentin, M., Zhao, R. & Goldman, I. D. The antifolates. *Hematol. Oncol. Clin. North Am.* **26**, 629–48, ix (2012).
 24. Zhou, W., Scocchera, E. W., Wright, D. L. & Anderson, A. C. Antifolates as effective antimicrobial agents: new generations of trimethoprim analogs. *Medchemcomm* **4**, 908 (2013).
 25. Adra, M. et al. Trimethoprim/sulfamethoxazole: evaluation of the available clinical and pharmacokinetic/pharmacodynamic evidence. *Ann. Pharmacother.* **38**, 1125–1133 (2011).
 26. Adra, M. & Lawrence, K. R. Trimethoprim/sulfamethoxazole for treatment of severe *Staphylococcus*

aureus infections. *Ann. Pharmacother.* **38**, 338–341 (2004).